
Figures and figure supplements

Temporal and thermal profiling of the *Toxoplasma* proteome implicates parasite Protein Phosphatase 1 in the regulation of Ca^{2+} -responsive pathways

Alice L Herneisen et al

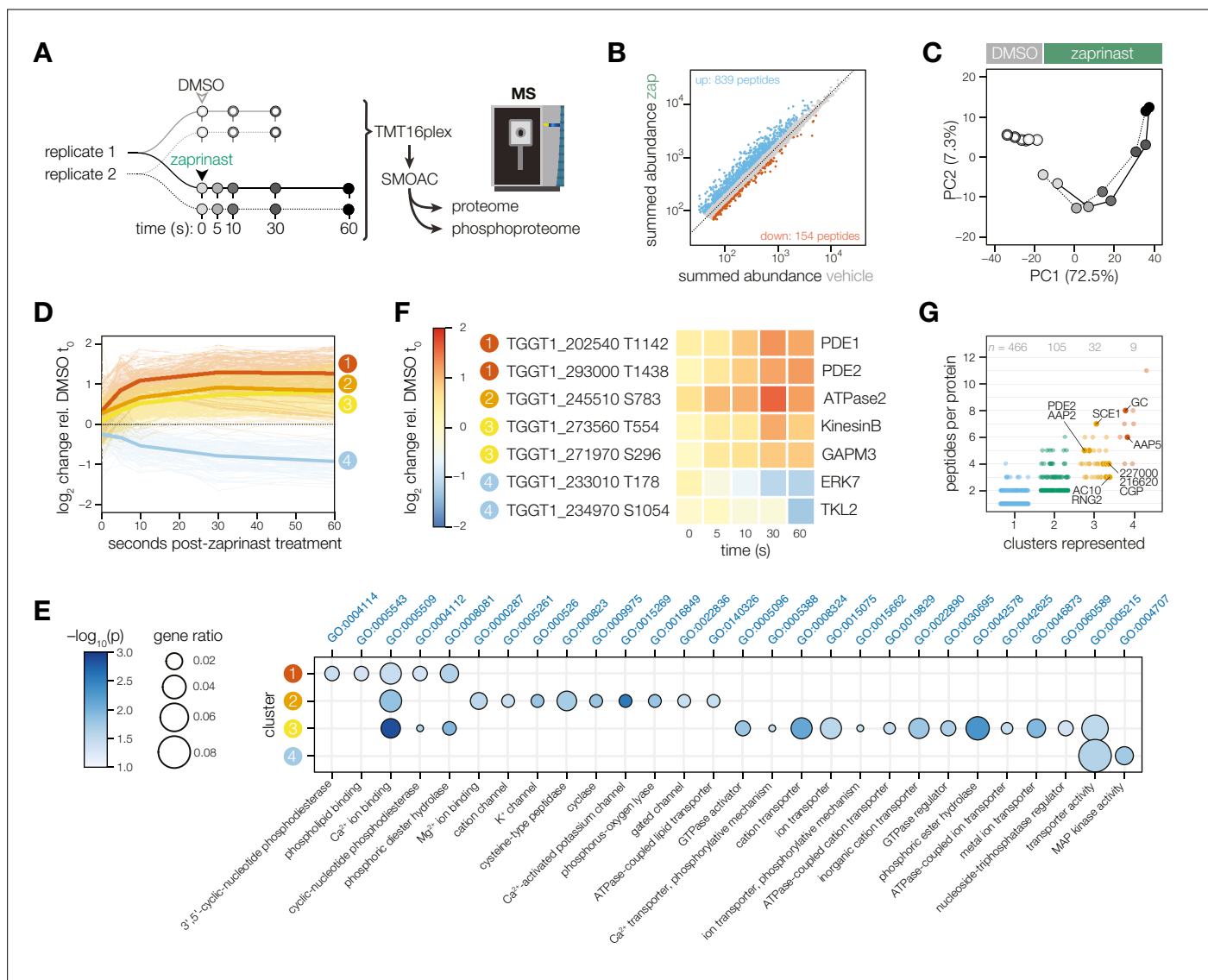


Figure 1. Phosphoregulation triggered by Ca^{2+} release. **(A)** Schematic of the sub-minute phosphoproteomics experiments with the Ca^{2+} signaling agonist zaprinast. **(B)** The summed abundances of unique phosphopeptides during zaprinast or vehicle (DMSO) treatment. The abundance ratios were transformed into a modified Z score and were used to threshold increasing ($Z > 3$; blue) or decreasing ($Z < -1.8$; orange) phosphopeptides. **(C)** Principal component analysis of phosphopeptides identified as significantly changing. Symbols follow the schematic in A. **(D)** Gaussian mixture-model-based clustering of phosphopeptides changing during zaprinast treatment. Solid lines show the median relative abundance of each cluster. Opaque lines show the individual phosphopeptides belonging to each cluster. **(E)** GO terms enriched among phosphopeptides changing with zaprinast treatment, grouped by cluster. Gene ratio is the proportion of proteins with the indicated GO term divided by the total number of proteins belonging to each cluster. Significance was determined with a hypergeometric test; only GO terms with $p < 0.05$ are shown. Redundant GO terms were removed. **(F)** Examples of phosphopeptides belonging to each cluster. **(G)** The number of clusters each phosphoprotein belongs to plotted against the number of changing phosphopeptides belonging to each protein. Gene names or IDs indicate proteins discussed in the text.

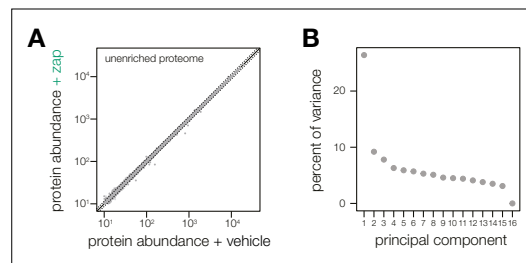


Figure 1—figure supplement 1. Metrics describing the zaprinast-dependent phosphoproteome. **(A)** Aggregate protein abundances for all time points from the non-phosphopeptide enriched samples of parasites treated with zaprinast or the corresponding vehicle (DMSO). Proteins quantified by a single peptide or more are shown in light and dark gray, respectively. Dotted lines correspond to two median absolute deviations. **(B)** Proportion of the variance explained by each principal component, as described in **Figure 1C**.

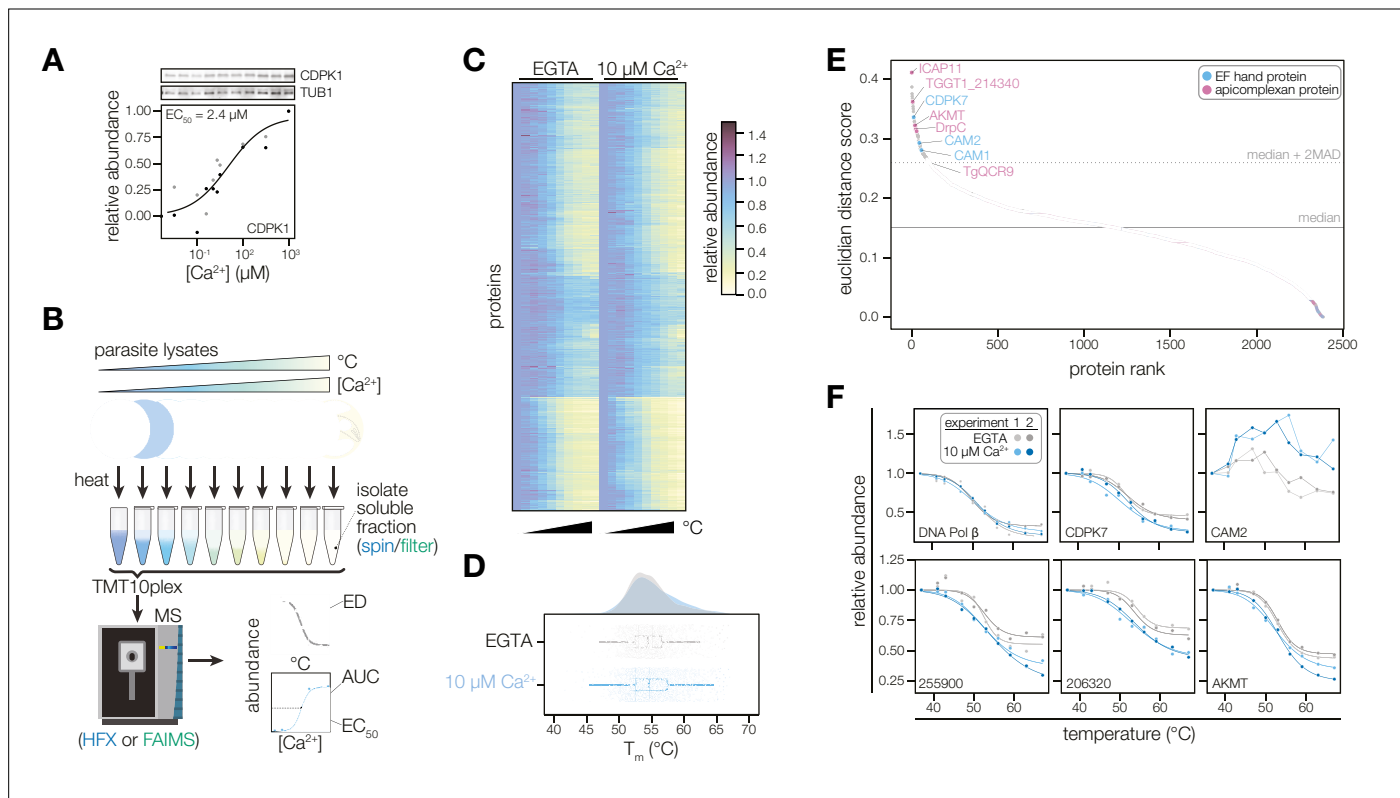


Figure 2. Thermal profiling identifies proteins that change stability in response to Ca²⁺. **(A)** Thermal shift assays can detect Ca²⁺-dependent stability of CDPK1 in extracts. Parasite lysates were combined with 10 concentrations of Ca²⁺ spanning the nanomolar to micromolar range. After denaturation at 58 °C, the soluble fraction was separated by SDS-PAGE and probed for CDPK1. Band intensity was normalized to the no-Ca²⁺ control and scaled. Points in shades of gray represent two different replicates. A dose-response curve was calculated for the mean abundances. **(B)** Schematic of the thermal profiling workflow. In the temperature-range experiment, parasite lysates were combined with EGTA or 10 μM [Ca²⁺]_{free} and heated at 10 temperatures spanning 37–67°C. In the concentration-range experiment, parasite lysates were combined with 10 different [Ca²⁺]_{free} (nM–mM range) and heated at 50, 54, or 58 °C. Temperature-range shifts were quantified by the Euclidean distance (ED) score, a weighted ratio of thermal stability differences between treatments and replicates. Concentration-range shifts were summarized by pEC₅₀, area under the curve (AUC), and goodness of fit (R²). **(C)** Heat map of protein thermal stability relative to the lowest temperature (37 °C) in 0 or 10 μM Ca²⁺. The mean relative abundance at each temperature was calculated for 2381 proteins. Proteins are plotted in the same order in both treatments. **(D)** Raincloud plots summarizing the distribution of T_m in lysates with EGTA (gray) or 10 μM [Ca²⁺]_{free} (blue). The average melting temperatures of proteins identified in two replicates were plotted. **(E)** Proteins rank-ordered by euclidean distance score quantifying the Ca²⁺-dependent shift in thermal stability. Solid and dotted lines represent the median ED score and two modified Z scores above the median, respectively. Highlighted proteins have EF hand domains (blue) or are conserved in apicomplexans (pink). **(F)** Thermal profiles of individual proteins: DNA polymerase β (TGTT1_233820); the EF hand domain-containing proteins CDPK7 (TGTT1_228750) and the calmodulin-like protein CAM2 (TGTT1_262010); potential Ca²⁺-leak channels TGTT1_255900 and TGTT1_206320; and AKMT (TGTT1_216080).

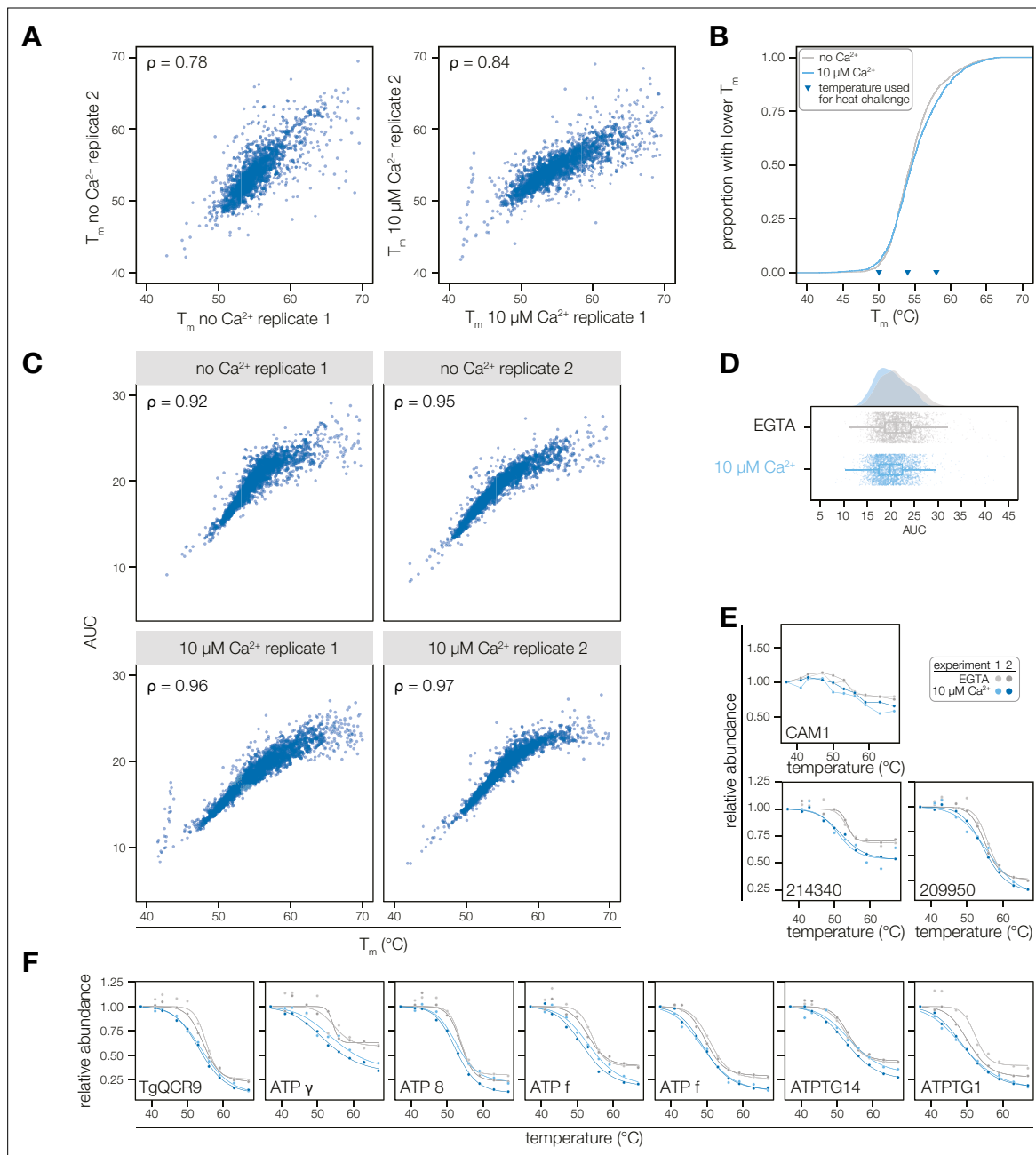


Figure 2—figure supplement 1. Extended data for thermal profiling experiments. **(A)** Comparison of the melting points of proteins with standard melting behavior ($R^2 > 0.8$) across replicate experiments and treatment conditions. The correlation of melting temperatures is given by Spearman's rho. **(B)** Cumulative distribution function of average measured melting temperatures in lysates with 10 μM or no Ca^{2+} . **(C)** Correlation between T_m of proteins with standard melting behavior ($R^2 > 0.8$) and AUC in each experiment. Correlation is given by Spearman's rho. **(D)** Distribution of AUC (as in Figure 1D). **(E)** Melting curve of proteins discussed in the text: CAM1 (TGGT1_246930), an ICAP (TGGT1_214340, Sidik et al., 2016a), and a putative thioredoxin (TGGT1_209950). **(F)** Melting curves of TgQCR9 and ATP synthase subunits (ATP) destabilized by Ca^{2+} .

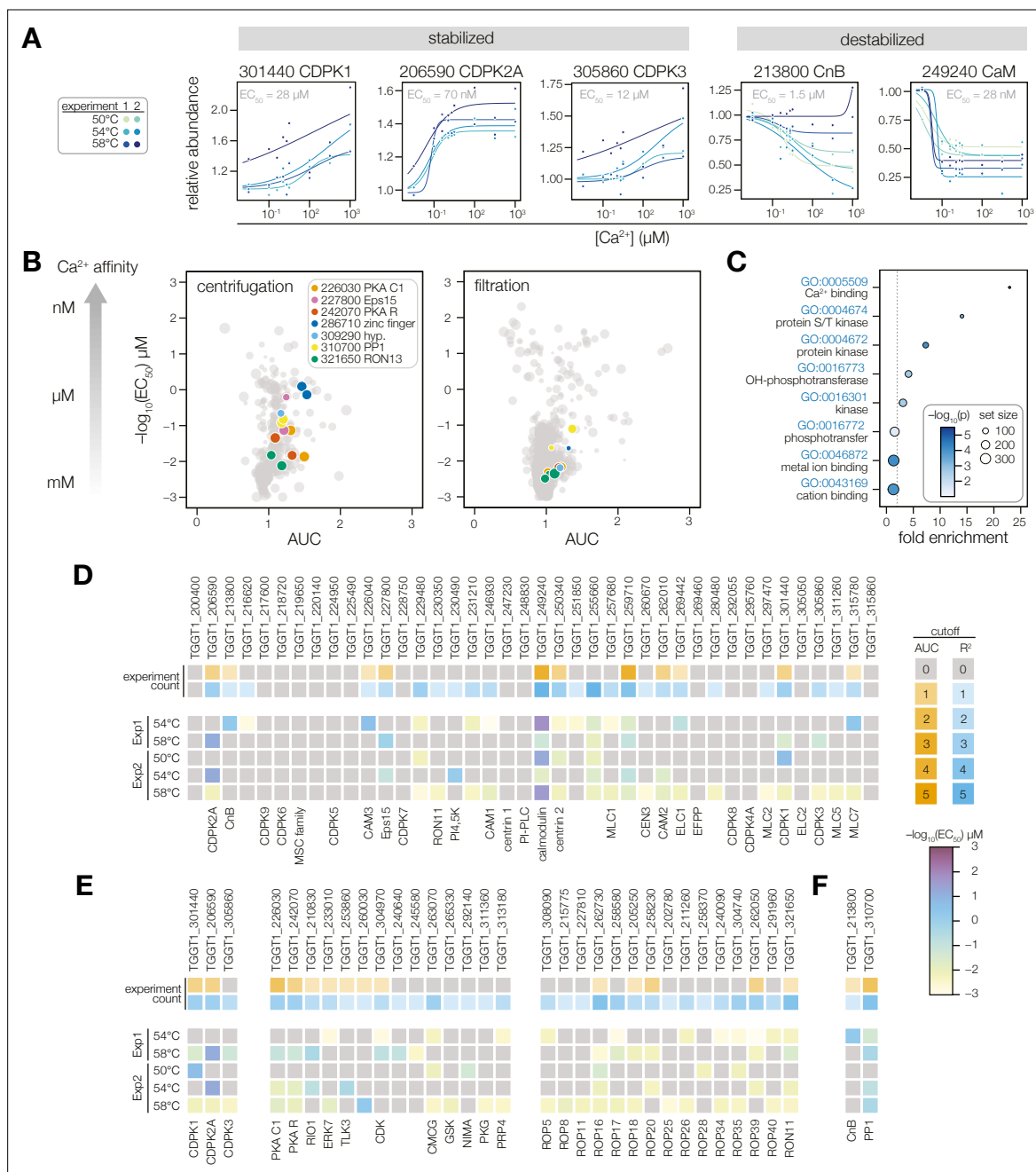


Figure 3. Thermal profiling identifies anticipated and unexplored Ca^{2+} -responsive proteins. **(A)** Mass spectrometry-derived thermal profiles of EF hand-containing proteins stabilized or destabilized by Ca^{2+} . Relative abundance is calculated relative to the protein abundance at 0 μM Ca^{2+} . EC_{50} is the median of the EC_{50} values of the curves displayed on the plots. **(B)** The magnitude of Ca^{2+} -dependent stabilization (AUC) plotted against the sensitivity (pEC_{50}) for protein abundances exhibiting a dose-response trend with an $R^2 > 0.8$. Point size is scaled to R^2 . Summary parameters for the different separation methods (ultracentrifugation or filtration) are plotted separately. Colors identify candidates with Ca^{2+} -responsive behavior validated in **Figure 4**. **(C)** Gene ontology (GO) terms enriched among candidate Ca^{2+} -responsive proteins (AUC greater than two modified Z scores and R^2 dose-response > 0.8). Fold enrichment is the frequency of Ca^{2+} -responsive proteins in the set relative to the frequency of the GO term in the population of detected proteins. Significance was determined with a hypergeometric test; only GO terms with $p < 0.05$ are shown. **(D–F)** EF hand domain proteins (**D**), protein kinases (**E**), and protein phosphatases (**F**) detected in the thermal profiling mass spectrometry datasets. The top rows indicate if a protein passed the AUC cutoff (orange) or R^2 cutoff (blue) for dose-response behavior. The opacity of the band represents the number of experiments in which the protein exhibited the behavior (out of five). The five rows below summarize the pEC_{50} of each experiment in which the protein exhibited a dose-response trend with $R^2 > 0.8$. Kinases are loosely grouped as CDPK's (included as a reference), non-rhoptry kinases, and secretory pathway kinases.

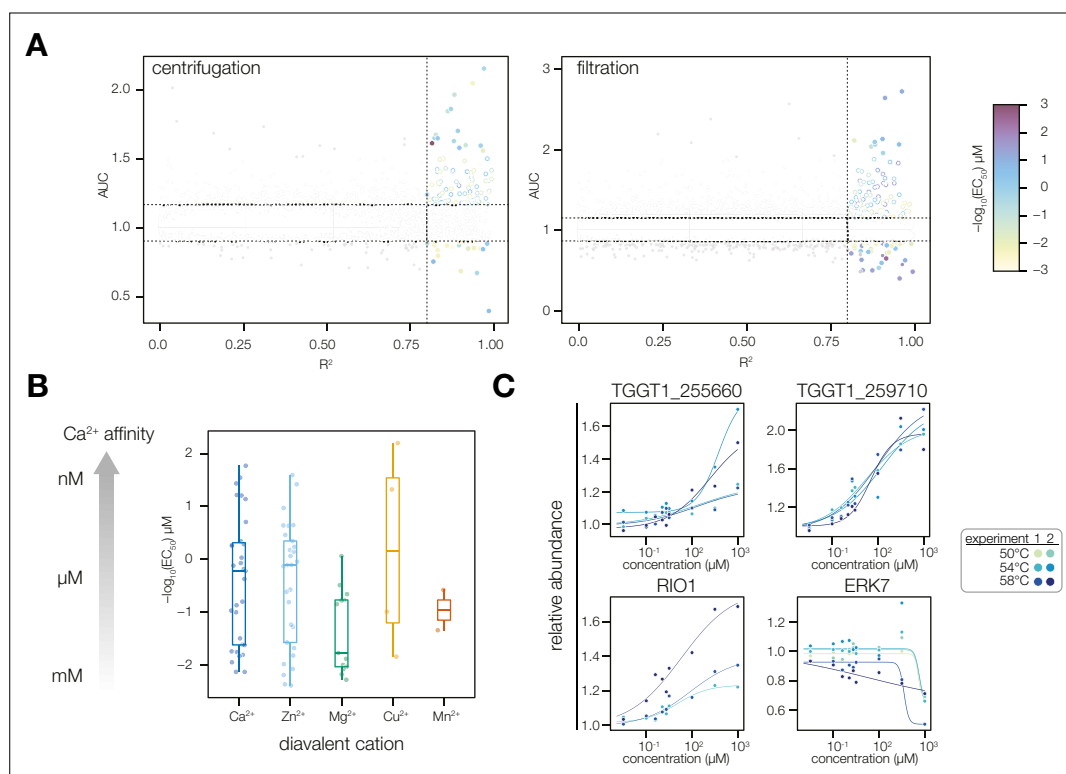


Figure 3—figure supplement 1. Extended analysis of thermal profiling experiments. **(A)** Plots of protein curve fit R^2 vs. AUC, a measure of stability change, for each set of MS experiments. Dotted lines indicate thresholds for designated Ca^{2+} -responsive behavior: $R^2 > 0.8$ and an AUC two modified Z scores from the median. Each point corresponds to an average of two replicates at each thermal challenge temperature (50, 54, or 58 °C). Color denotes pEC_{50} in μM . **(B)** A comparison of the pEC_{50} values of proteins predicted to bind different divalent metal cations. Specificity was predicted via the presence of Interpro domains and through manual annotation. **(C)** Plots of individual protein melting curves, as described in the text: the EF hand domain-containing proteins TGGT1_255660 and TGGT1_259710; and the kinases RIO1 (TGGT1_210830) and ERK7 (TGGT1_233010).

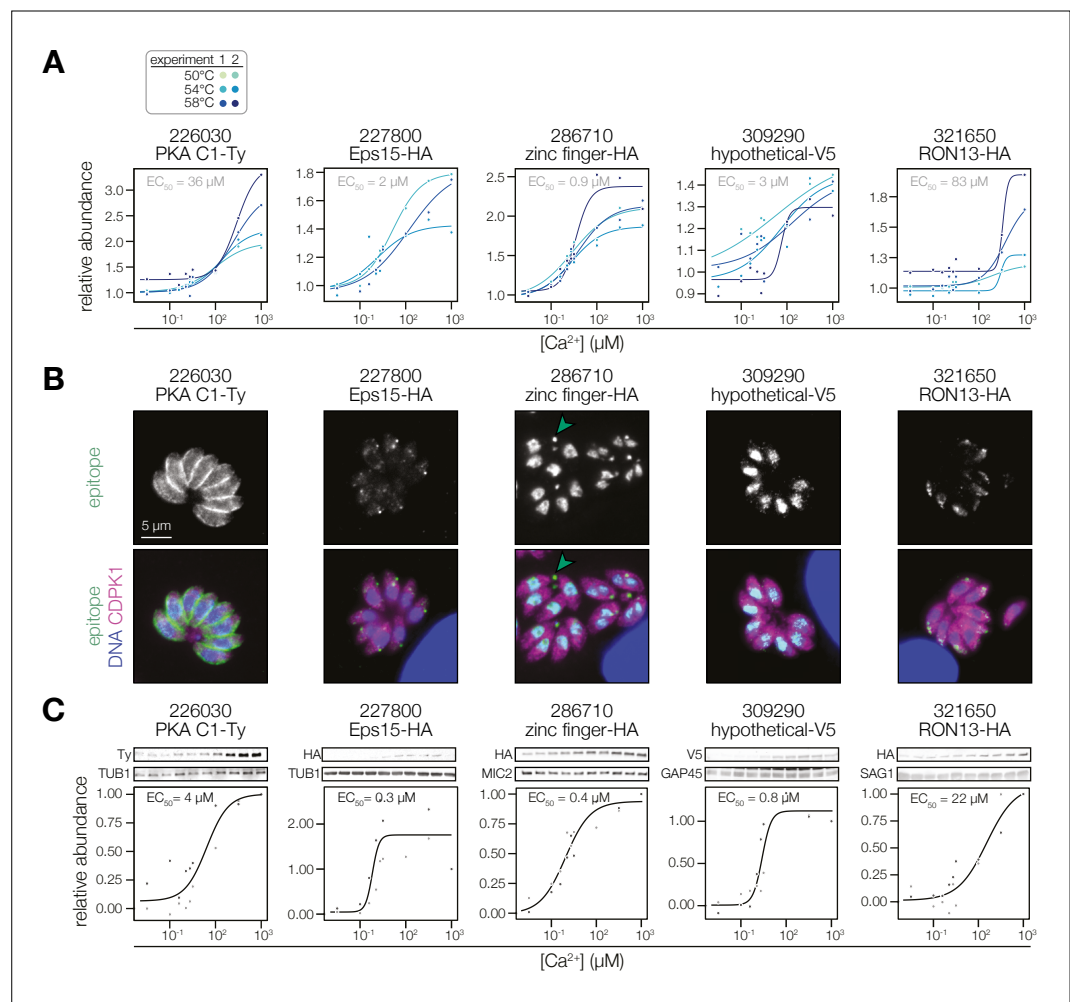


Figure 4. Validation of Ca^{2+} -dependent thermal stability. **(A)** Mass spectrometry-derived thermal profiles of the candidates, as in **Figure 3A**. **(B)** Immunofluorescence images of fixed intracellular parasites expressing the indicated proteins with C-terminal epitopes at endogenous loci. Hoechst and anti-CDPK1 were used as counterstains in the merged image. Green arrowheads highlight an example of TGGT1_286710 residual body staining. In the case of PKA C1/R, the stain of the R subunit is shown, as both subunits colocalize. **(C)** Immunoblot-derived thermal profiles of the candidates. Colors correspond to two independent replicates. Uncropped blots are shown in the **Figure 4—figure supplement 1**.

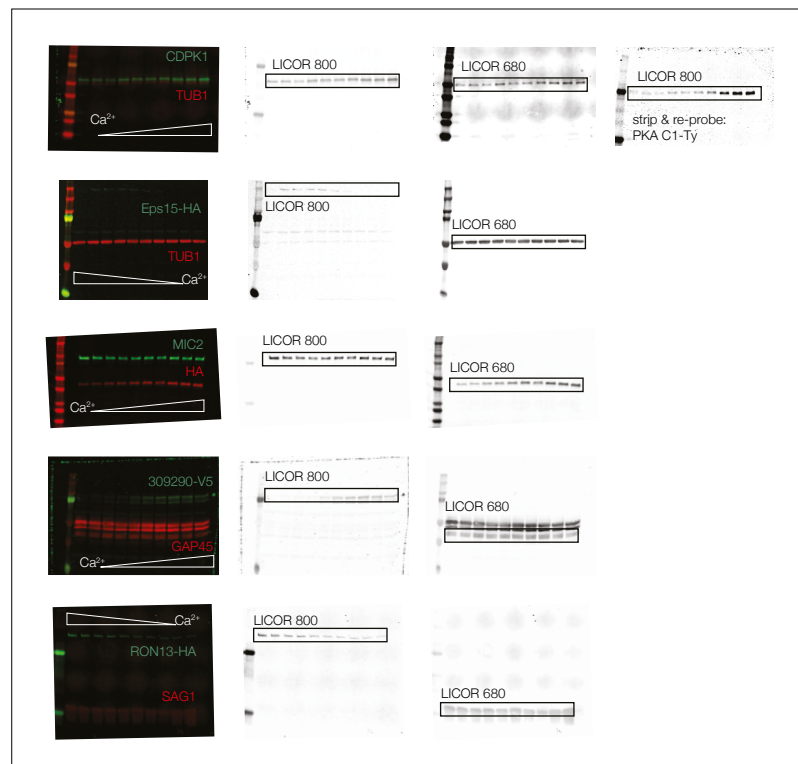


Figure 4—figure supplement 1. Uncropped immunoblots, as in **Figure 4C**. Parasite lysates were incubated at 10 Ca^{2+} concentrations and were thermally challenged at 58 °C. Following centrifugation, the supernatant containing the soluble protein fraction was separated by SDS-PAGE. Following transfer onto a nitrocellulose membrane, the blots were probed with the indicated primary antibodies. The direction of the Ca^{2+} gradient is indicated on each blot. Representative blots from two biological replicates are shown.

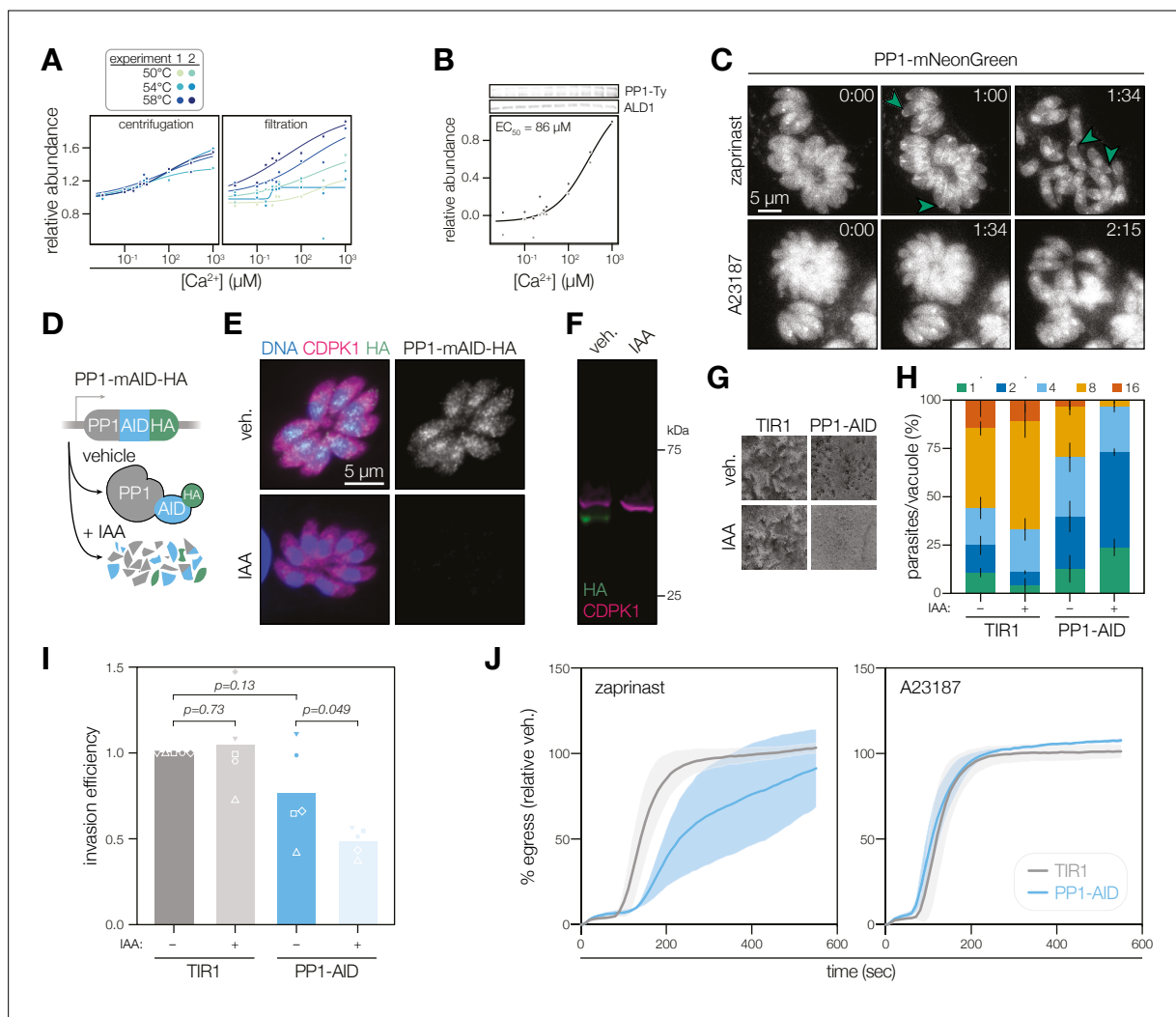


Figure 5. PP1 is a Ca²⁺-responsive enzyme involved in *T. gondii* egress and invasion. **(A)** The Ca²⁺-dependent stabilization of PP1 (TGGT1_310700) in each mass spectrometry experiment. **(B)** Immunoblotting for endogenously tagged PP1-mNG-Ty at different Ca²⁺ concentrations and thermal challenge at 58 °C. Abundance is calculated relative to the band intensity at 0 μM Ca²⁺ and scaled. Points in shades of gray represent different replicates. A dose-response curve was calculated for the mean abundances. **(C)** Parasites expressing endogenously tagged PP1-mNG egress after treatment with 500 μM zaprinast or 4 μM A23187. Arrows show examples of PP1 enrichment at the apical end. Time after treatment is indicated in m:ss. **(D)** Rapid regulation of PP1 by endogenous tagging with mAID-HA. IAA, Indole-3-acetic acid (IAA). **(E)** PP1-mAID-HA visualized in fixed intracellular parasites by immunofluorescence after 3 hr of 500 μM IAA or vehicle treatment. Hoechst and anti-CDPK1 are used as counterstains (Waldman et al., 2020). **(F)** PP1-mAID-HA depletion, as described in (E), monitored by immunoblotting. The expected molecular weights of PP1-mAID-HA and CDPK1 are 48 and 65 kDa, respectively. **(G)** Plaque assays of 1,000 TIR1 and PP1-mAID-HA parasites infected onto a host cell monolayer and allowed to undergo repeated cycles of invasion, replication, and lysis for 7 days in media with or without IAA. **(H)** The number of parasites per vacuole measured for PP1-mAID-HA and the TIR1 parental strain after 24 hr of 500 μM IAA treatment. Mean counts (n=3) are expressed as a percentage of all vacuoles counted. **(I)** Invasion assays PP1-mAID-HA or TIR1 parental strains treated with IAA or vehicle for 3 hr. Parasites were incubated on host cells for 60 min prior to differential staining of intracellular and extracellular parasites. Parasite numbers were normalized to host cell nuclei for each field. Means graphed for n=5 biological replicates (different shapes), Welch's t-test. **(J)** Parasite egress stimulated with 500 μM zaprinast or 8 μM A23187 following 3 h of treatment with vehicle or IAA. Egress was monitored by the number of host cell nuclei stained with DAPI over time and was normalized to egress in the vehicle-treated strain. Mean ±S.D. graphed for n=3 biological replicates.

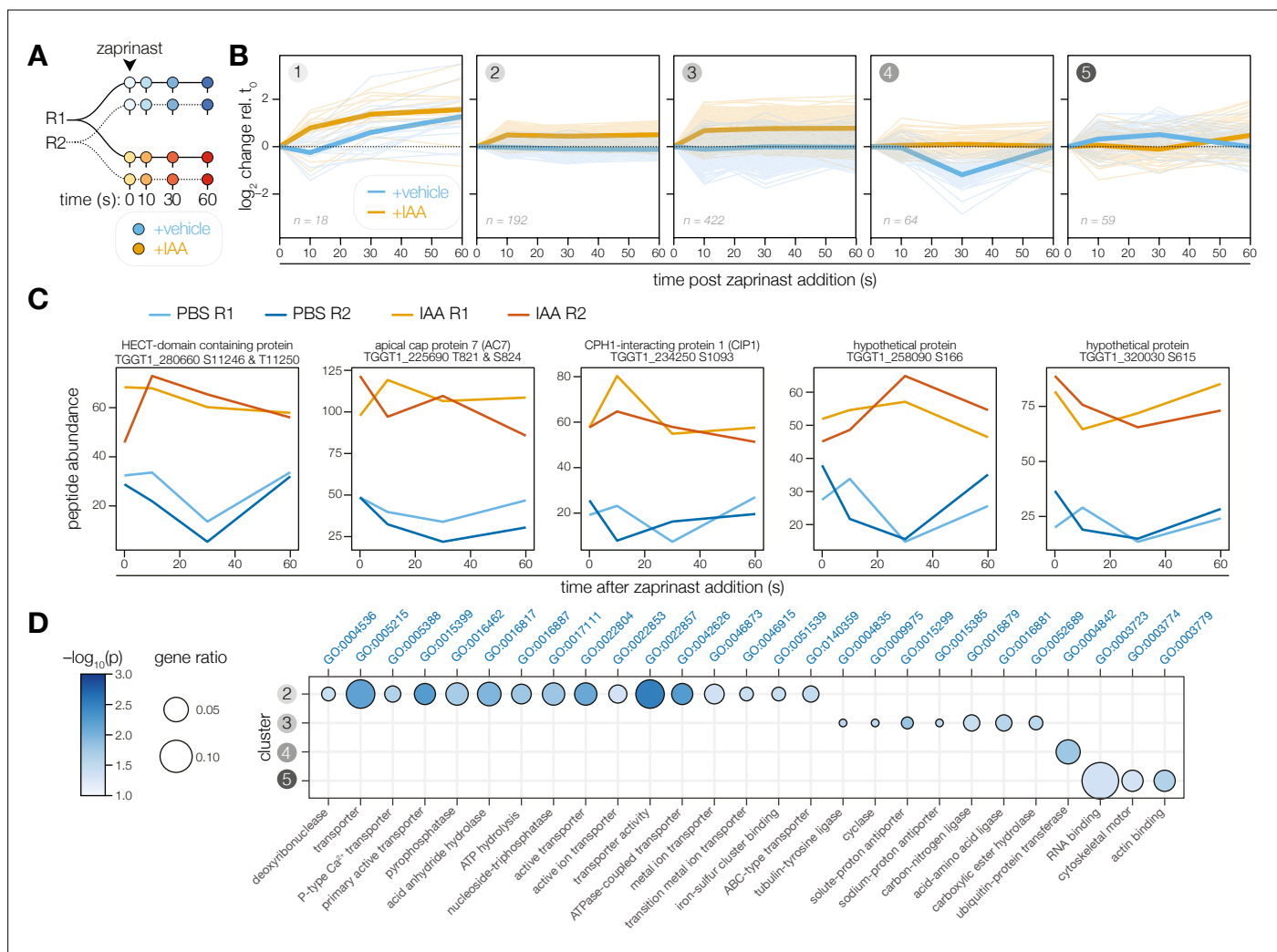


Figure 6. The PP1-dependent phosphoproteome. **(A)** Schematic of the phosphoproteomics time course. PP1-AID parasites were treated with IAA or vehicle for 3 hr. Extracellular parasites were then treated with zaprinast, and samples were collected during the first minute after stimulation. The experiment was performed in biological replicate (R1 and R2). **(B)** Five clusters were identified with respect to phosphopeptide dynamics and PP1-dependence. **(C)** Examples of phosphopeptides dynamically regulated by zaprinast and exhibiting PP1-dependent dephosphorylation. **(D)** GO terms enriched among phosphopeptides, grouped by cluster. Gene ratio is the proportion of proteins with the indicated GO term divided by the total number of proteins belonging to each cluster. Significance was determined with a hypergeometric test; only GO terms with $p < 0.05$ and represented by more than one protein are shown. Redundant GO terms were removed. Cluster 1 lacked enough peptides for enrichment analysis.

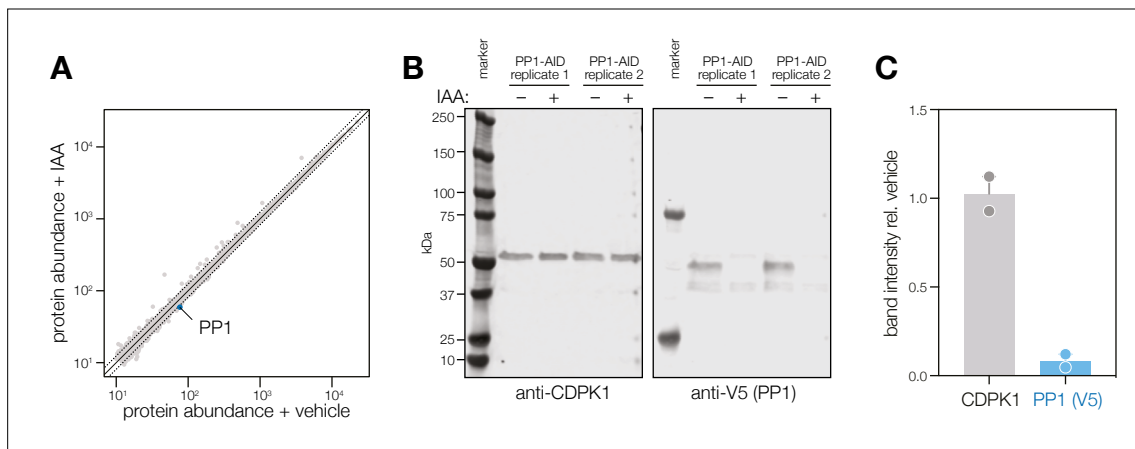


Figure 6—figure supplement 1. Extended analysis of PP1 phosphoproteomics experiment. **(A)** Aggregate protein abundances from the non-phosphopeptide enriched samples of parasites treated with IAA or vehicle. Proteins quantified by a single peptide or more are shown in light and dark gray, respectively. Lines correspond to two median absolute deviations. **(B)** Immunoblot of samples used for the PP1 phosphoproteomics experiment. **(C)** Quantification of immunoblot band intensity. Intensity was normalized relative to the signal of the vehicle-treated lane for each replicate. Mean \pm SD plotted for two independent replicates.

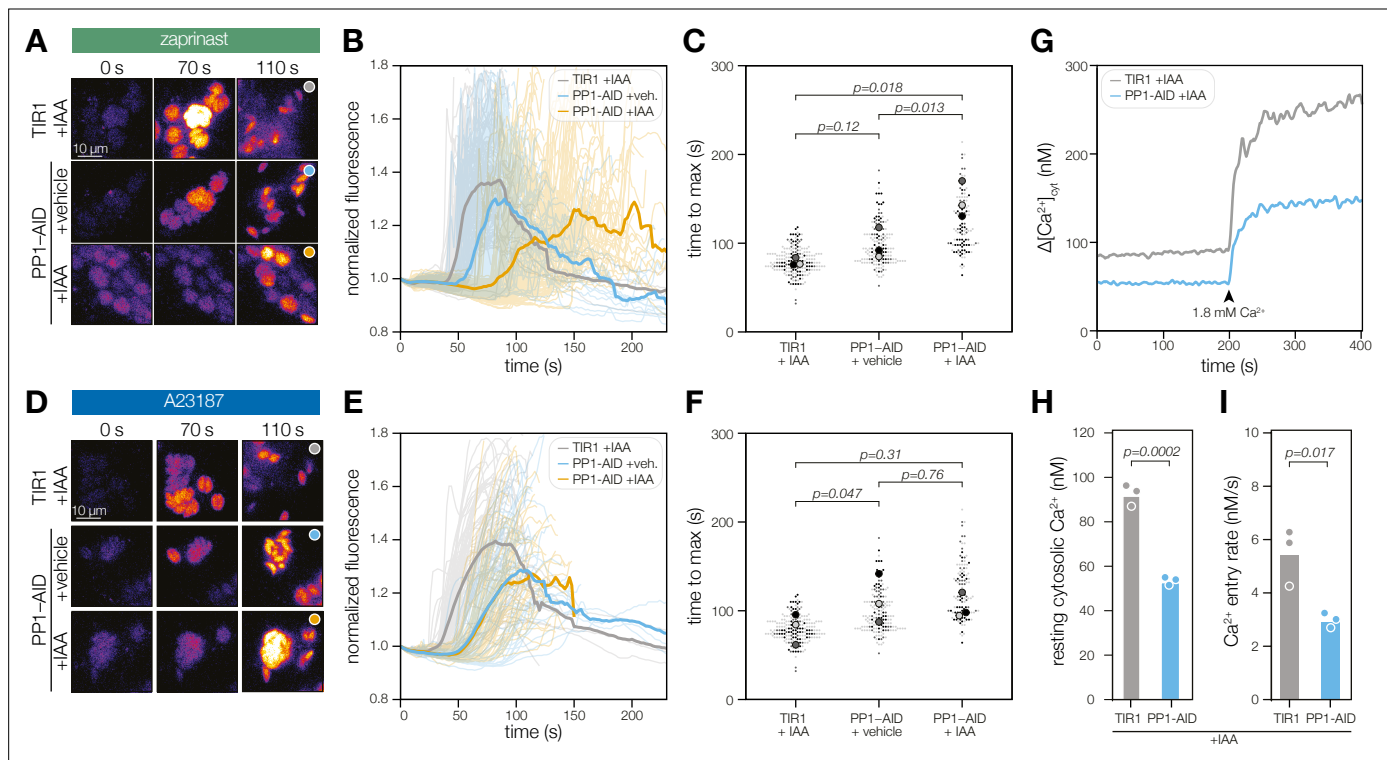


Figure 7. PP1 ensures rapid Ca^{2+} mobilization prior to zaprinast-induced egress. **(A)** Selected frames of time-lapse images of PP1-AID parasites expressing the genetically encoded Ca^{2+} indicator GCaMP following treatment with 500 μ M zaprinast. **(B)** Normalized GCaMP fluorescence of individual vacuoles was tracked after zaprinast treatment and prior to egress (opaque lines). The solid line represents the mean normalized fluorescence of all vacuoles across $n=3$ biological replicates. **(C)** The time to maximum normalized fluorescence of individual vacuoles after zaprinast treatment. Different replicates are shown in different shades of gray. Small points correspond to individual vacuoles; large points are the mean for each replicate. p Values were calculated from a two-tailed t-test. **(D)** Selected frames of time-lapse images of PP1-AID parasites expressing the genetically encoded Ca^{2+} indicator GCaMP following treatment with 4 μ M A23187. **(E)** Normalized GCaMP fluorescence of individual vacuoles was tracked after A23187 treatment and prior to egress (opaque lines). The solid line represents the mean normalized fluorescence of all vacuoles across $n=3$ biological replicates. **(F)** The time to maximum normalized fluorescence of individual vacuoles after A23187 treatment. Small points correspond to individual vacuoles; large points are the mean for each replicate. p Values were calculated from a two-tailed t-test. **(G)** Fluorescence intensity of Fura2/AM-loaded TIR1 or PP1-AID parasites treated with IAA for 5 hr before and after addition of the 1.8 mM Ca^{2+} . Representative traces from three biological replicates. **(H)** Resting cytoplasmic $[Ca^{2+}]$ prior to incubation in buffers with elevated $[Ca^{2+}]$. p Values were calculated from an ANOVA. **(I)** The rate of Ca^{2+} entry in the first 20 s after addition of 1.8 mM Ca^{2+} to parasites p values were calculated from an ANOVA. Entry rates following addition of other concentrations are shown in **Figure 7—figure supplement 1**.

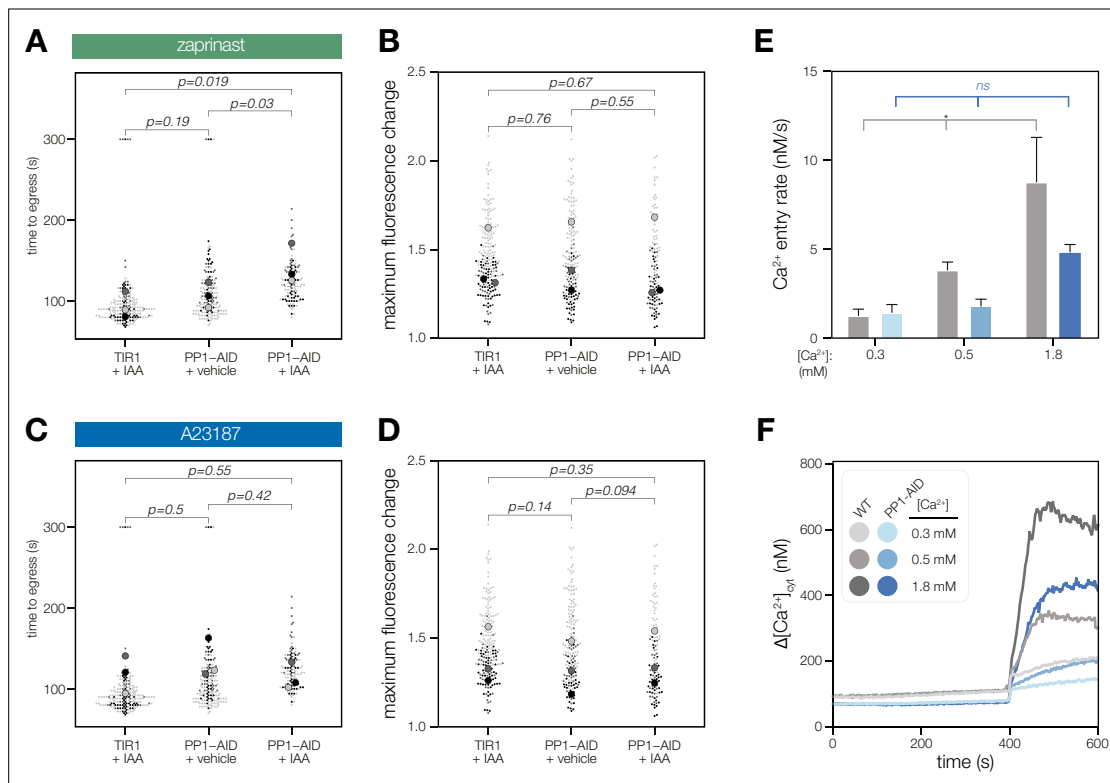


Figure 7—figure supplement 1. PP1-AID parasites egress, as quantified by video microscopy. **(A)** The time to vacuole egress after zaprinast treatment was manually scored. Different replicates are shown in different shades of gray. Small points represent individual vacuoles; large points are the mean for each replicate. p Values were calculated from a two-tailed t-test. **(B)** The normalized fluorescence change of individual vacuoles after zaprinast treatment. Different replicates are shown in different shades of gray. Small points correspond to individual vacuoles; large points are the mean for each replicate. p Values were calculated from a two-tailed t-test. **(C)** The time to vacuole egress after A23187 treatment was manually scored. Different replicates are shown in different shades of gray. Small points correspond to individual vacuoles; large points are the mean for each replicate. p Values were calculated from a two-tailed t-test. **(D)** The normalized fluorescence change of individual vacuoles after A23187 treatment. Different replicates are shown in different shades of gray. Small points represent individual vacuoles; large points are the mean for each replicate. p Values were calculated from a two-tailed t-test. **(E)** Ca²⁺ entry rates corresponding to **(F)**. The slope of the trace at the time of addition of Ca²⁺ was measured as the change in the concentration of Ca²⁺ during the initial 20 s after addition of Ca²⁺. Each bar represents the average of a minimum of three biological replicates. ANOVA was used for the statistical analyses. * $p < 0.01$. **(F)** Fluorescence intensity of Fura2/AM-loaded TIR1 or PP1-AID parasites treated with IAA for 5 hours upon incubation with buffers of the indicated [Ca²⁺]. Representative traces from at least three biological replicates.